



Proteomic analysis for busulfan-induced spermatogenesis disorder

Ke Hu^a , Qinran Zhu^a, Jiaqi Zou^a, Xin Li^a, Min Ye^a, Jing Yang^a, Sixieyang Chen^a, Fan Li^b, Biao Ding^c, Shuai Yang^c, Chuanwang Song^b and Meng Liang^a 

^aSchool of Life Science, Bengbu Medical University, Bengbu, China; ^bSchool of Laboratory Medicine, Bengbu Medical University, Bengbu, China; ^cFirst Affiliated Hospital, Bengbu Medical University, Bengbu, China

ABSTRACT

Background: Busulfan is the most commonly used drug for the treatment of chronic myelogenous leukemia and pretreatment for hematopoietic stem cell transplantation, which can damage the reproductive and immune system. However, little is known about the protein expression profiling in busulfan treated testis.

Methods: This research studies the proteomics for busulfan-induced spermatogenesis disorder. The model of busulfan-induced mouse spermatogenesis disorder was subjected to label-free quantification proteomics analysis. Clustering heatmap, gene ontology, Kyoto Encyclopedia of Genes and Genomes (KEGG) pathway and protein interaction analyses were performed and validated by molecular experiments.

Results: The busulfan-treated mouse model showed abnormal testis morphology and reduced sperm number and testis weight. Testicular and sperm damage was most severe at 30 days after busulfan treatment. The busulfan-treated mouse testes were subjected to label-free quantification proteomics, which revealed 190 significantly downregulated proteins including lactate dehydrogenase A like 6B (LDHAL6B) and ubiquitin-specific protease 7 (USP7). In addition, the testis and spermatozoa in the epididymis progressively improved from 70 to 80 days after busulfan treatment, and that the testis weight and spermatozoa number gradually increased from 40 to 80 days after busulfan treatment. Western blotting revealed that LDHAL6B protein significantly increased at 10 days, decreased from 20 to 60 days, and then gradually elevated from 70 to 80 days after busulfan treatment.

Conclusion: We revealed 190 significantly downregulated proteins in busulfan-treated mouse testes at 30 days and indicated that 70 days is the cut-off point of spermatogenic recovery for busulfan-treated mouse testis, increasing our understanding of this reproductive disorder model. An increased understanding of busulfan's toxic effect will help to prevent and treat reproductive diseases.

ARTICLE HISTORY

Received 25 July 2023
Revised 5 November 2024
Accepted 8 November 2024

KEYWORDS





Proteomic analysis;
busulfan;
spermatogenesis; testis


Introduction

Clinically, busulfan is the most commonly used drug for the treatment of chronic myelogenous leukemia and pretreatment for hematopoietic stem cell transplantation, but can damage the reproductive and immune system [1,2]. Injection of pregnant rats with busulfan can lead to developmental disorders of the central nervous system in the pups [3]. Human amnion mesenchymal stem cells can resist busulfan-induced spermatogenesis disorder, with a reduction in cell apoptosis, increased cell proliferation and lower amounts of oxidative damage [4], which mean that toxic effect of busulfan can be recovered by the body its self. Alginate oligosaccharides can restore

busulfan-induced spermatogenesis disorder by improving spermatogenic development and the testicular tissue microenvironment [5]. The protein expression level of phosphoribosyl-pyrophosphate synthetase 2 (PRPS2) is significantly reduced in busulfan-induced spermatogenesis disorder mouse testis and knockdown of *Prps2* promotes germ cell apoptosis [6]. Thus, understanding of the proteomics in busulfan-induced spermatogenesis disorder will be helpful for the treatment of male infertility.

The clinical use of busulfan in the treatment of special diseases can cause a series of side effects of reproductive disorders. We wanted to know through what protein pathway the reproductive side effects of

CONTACT Meng Liang  lmhk@mail.ustc.edu.cn  School of Life Science, Bengbu Medical University, 2600 Donghai Avenue, Bengbu 233030, Anhui Province, China; Chuanwang Song  bbmcscw@foxmail.com  School of Laboratory Medicine, Bengbu Medical University, 2600 Donghai Avenue, Bengbu 233030, Anhui Province, China.

 Supplemental data for this article can be accessed online at <https://doi.org/10.1080/07853890.2024.2442534>.

© 2024 The Author(s). Published by Informa UK Limited, trading as Taylor & Francis Group

This is an Open Access article distributed under the terms of the Creative Commons Attribution-NonCommercial License (<http://creativecommons.org/licenses/by-nc/4.0/>), which permits unrestricted non-commercial use, distribution, and reproduction in any medium, provided the original work is properly cited. The terms on which this article has been published allow the posting of the Accepted Manuscript in a repository by the author(s) or with their consent.

busulfan affect spermatogenesis. In addition, we speculated that these side effects of busulfan might disappear over time. The further study on the reproductive side effects and spermatogenesis recovery can provide reference value for clinical rational use of busulfan. In this study, the busulfan-induced spermatogenesis disorder mouse testes were subjected to label-free quantification proteomics and clustering heatmap, gene ontology, Kyoto Encyclopedia of Genes and Genomes (KEGG) pathway and protein interaction analyses.

Methods

Construction of busulfan-induced spermatogenesis disorder mouse model

Institute of cancer research of American (ICR) mice were derived from two male and seven female albino Swiss mice from a non-inbred stock in the laboratory of Dr. de Coulon at the Centre Anticancereux Romand in Switzerland [7] and purchased from Skbex Biotechnology Co., Ltd (Anyang, Henan, China). Male ICR mice (2 months old) were injected intraperitoneally once with 30 mg/kg busulfan (Merck KGaA, Darmstadt, Germany) according to body weight or the vehicle alone, and then the mice were studied after 10, 20, 30, 40, 50, 60, 70 and 80 days which were set four mice in each group and repeated three times. Mice were sacrificed by carbon dioxide asphyxiation followed by cervical dislocation, which were weighed and disinfected with 75% alcohol (Lircon, Dezhou, China). The abdomen of the sacrificed mice was opened through surgical scissor, and then testes and epididymes were pulled from the scrotum, dissected free of surrounding tissue and weighed. Separated testes and epididymes were used for morphological imaging, H&E staining of sections, spermatozoa counting, or protein detecting. For H&E staining, testicular and epididymal tissues were incubated in 4% paraformaldehyde (MACLIN, Shanghai, China) for 24 h, dehydrated, and embedded in paraffin (Shanghai Huayong Paraffin Wax Co., LTD, Shanghai, China) using a previously described protocol [8]. The paraffin-embedded tissues were cut into 5 μ m sections, which were mounted on glass slides, dewaxed, and rehydrated. The sections were then stained with H&E (Servicebio, Wuhan, China), dehydrated and sealed with neutral gum (Sinopharm Chemical Reagent Co., LTD, Shanghai, China). Finally, the slides were observed under a light microscope and photographed. To count the spermatozoa, the whole epididymis was clipped in 10 mL PBS (Gibco, Thermo Fisher Scientific, Waltham, MA, USA) and incubated at 37°C for 20 min. Spermatozoa from the entire epididymis were released and then counted under a microscope using a cell counting plate.

Proteomic analysis of busulfan-treated testis

Busulfan-treated testis was separated from the mouse body and isolated proteins were subjected to label-free quantification proteomics (Aksomics Biotechnology Co., Ltd., Shanghai, China) [9]. Briefly, busulfan-treated testis was separated from the mouse body and proteins were extracted from testis using RIPA (25 mM Tris-HCl pH 7.6 (Sigma-Aldrich, Saint Louis, MO, USA), 150 mM NaCl (Sangon Biotech, Shanghai, China), 1% NP-40 (Sangon Biotech), 1% sodium deoxycholate (Sigma-Aldrich), 1% SDS (Sangon Biotech)) supplemented with protease inhibitors inhibitor cocktail (Kangchen Biotech, Shanghai, China) and PMSF (Sigma-Aldrich). Protein concentration was determined by BCA protein assay kit (Pierce, Rockford, IL, USA). Take 100 μ g proteins and add prechilled acetone (Sangon Biotech) to alkylated proteins. Extracted proteins were solubilized in 100 mM ammonium bicarbonate (Sigma-Aldrich) with 1% sodium deoxycholate and reduced by 5 mM tris (2-carboxyethyl) phosphine hydrochloride (Sigma-Aldrich) for 10 min at 55°C, followed by alkylation with 10 mM iodoacetamide (Sigma-Aldrich) for 15 min in the dark at room temperature. The proteins were then digested overnight at 37°C with sequencing grade modified trypsin (trypsin 1:50 protein w/w ratio; Promega, Madison, WI, USA). After clean-up of SDC with 2% trifluoroacetic acid (Sigma-Aldrich), the tryptic peptides were desalted using C18 columns (3M) (Sigma-Aldrich) and the eluted peptides were dried with vacuum concentrator (Thermo Fisher Scientific). Above peptides were separated by nano-UPLC liquid phase system EASY-nLC1200 (Thermo Fisher Scientific) and then analyzed using Q-Exactive mass spectrometer (Thermo Fisher Scientific). Raw data were processed with MaxQuant software (version 1.6.1.0) (Max Planck Institute of Biochemistry, Martinsried, Germany). Differentially regulated proteins were identified using the standard of fold change ≥ 2 and p value ≤ 0.05 , and were plotted in a volcano plot and clustering heatmap. The differentially expressed proteins in busulfan-treated mouse testis were predicted by gene ontology including biological process, cellular component and molecular function [10–12] and KEGG pathway analysis [13,14]. Finally, protein interactions following busulfan treatment were predicted using the search tool for the retrieval of interacting genes (STRING) database to show potential pathways of differentially expressed protein [15,16].

Western blotting and immunofluorescence

For western blotting, total protein was isolated from testicular tissues using RIPA (Millipore, Bedford, MA, USA) according to manufacturer's instruction, measured by

Enhanced BCA Protein Assay Kit (Beyotime, Shanghai, China), separated by SDS-PAGE (Beyotime) electrophoresis, transferred to nitrocellulose membrane (Pall Corporation, Show Low, AZ, USA), and then incubated with primary antibodies for LDHAL6B (ABclonal Technology, Wuhan, China) and β -actin (ABclonal Technology) and secondary antibody (ABclonal Technology). Protein levels were quantified using Image Lab software version 3.0 (Bio-Rad, Hercules, CA, USA). For immunofluorescence, testicular tissues were first fixed with 4% paraformaldehyde and then paraffin-embedded and sectioned. Immunofluorescence for LDHAL6B protein was detected using a previously described protocol [17]. 4',6-diamidino-2-phenylindole (DAPI) (Servicebio) and fluorescent secondary antibody (Servicebio) were purchased from Servicebio.

Statistical analysis

All experiments in this study were conducted independently at least three times. Data is displayed as

mean \pm standard error of the mean (SEM) and was analyzed with Student's t-test using GraphPad Prism 8 (Graph Pad Software Inc., La Jolla, CA, USA). $p < 0.05$ was regarded as a significant difference.

Results

Most spermatocytes and spermatids disappeared in busulfan-induced spermatogenesis disorder mouse testis

The model of busulfan-induced mouse spermatogenesis disorder was used to study the protein expression in male infertility. 10, 20 and 30 days after busulfan treatment, hematoxylin and eosin (H&E) staining showed that damage to the testis and spermatozoa in the epididymis progressively worsened, which included vacuoles, cell sloughing, multinucleated giant cells, disappearance of most spermatocytes and spermatids, and spermatid retention (Figure 1A). Weight detecting demonstrated that the testicular weight gradually

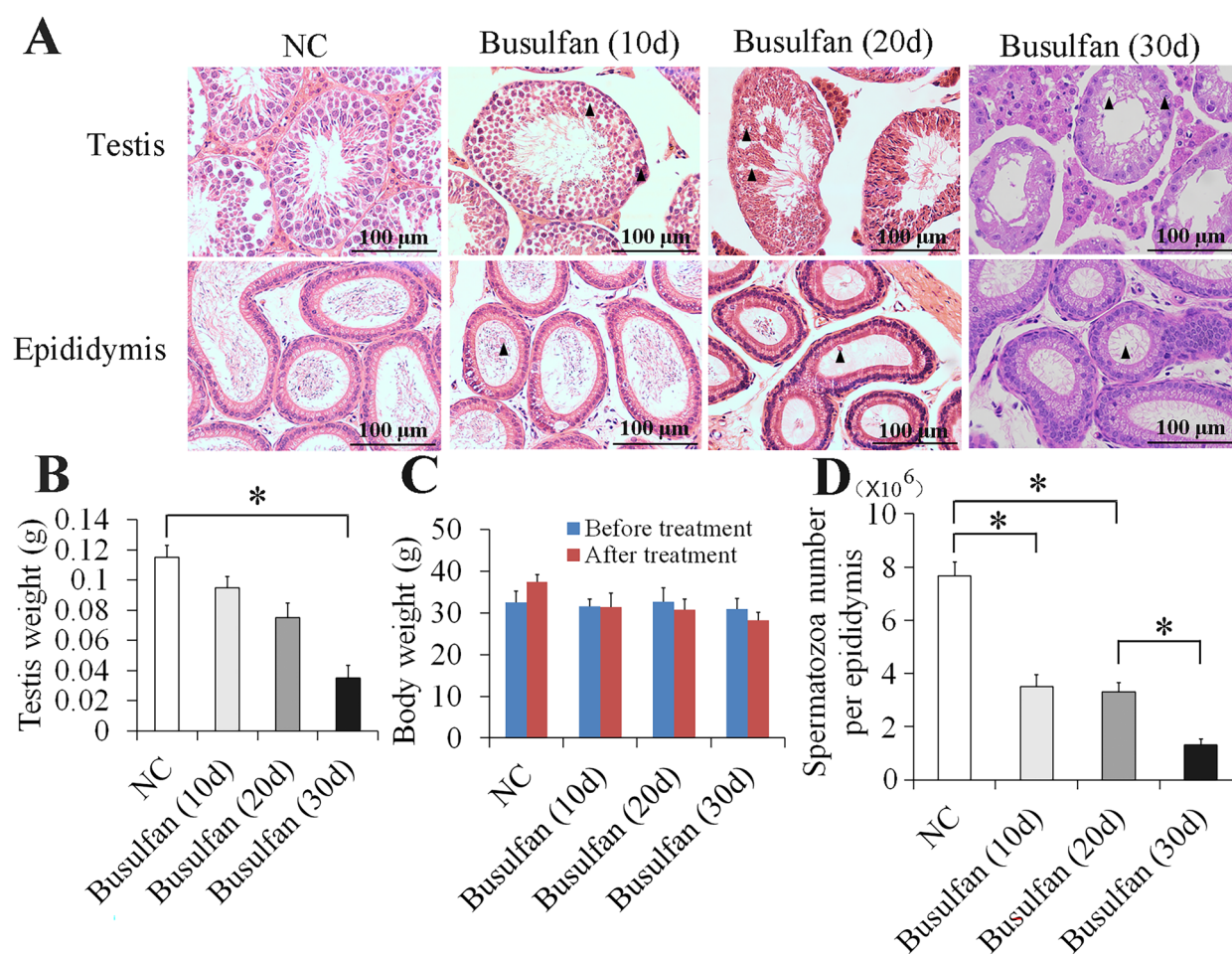


Figure 1. Obvious damage of testis and spermatozoa in epididymis appeared at 30 days after busulfan treatment. Mice were injected intraperitoneally once with busulfan, and then testes and epididymides were separated for H&E staining (A) and measurement of testis weight (B) and spermatozoa number (D) after 10, 20 and 30 days treatment. Arrow heads indicate abnormal germ cells (A). Body weight was also recorded before and after busulfan treatment (C). NC, negative control; $*p < 0.05$.

decreased from 10 to 30 days after busulfan treatment (Figure 1B) and body weight didn't change significantly from 10 to 30 days before and after busulfan treatment (Figure 1C). In addition, spermatozoa counting revealed that spermatozoa number also gradually decreased from 10 to 30 days after busulfan treatment (Figure 1D). Testicular and spermatogenic damage was most severe on 30 days after busulfan treatment (Figure 1A–D). These results proved that busulfan can prompt the disappearance of most spermatocytes and spermatids in busulfan-induced mouse spermatogenesis disorder.

Proteomic analysis of busulfan-induced spermatogenesis disorder mouse testis

We next identified which proteins are involved in disappearance of most spermatocytes and spermatids in the busulfan-induced spermatogenesis disorder model. 30 days after busulfan treatment the mouse testes were subjected to label-free quantification proteomics, and a volcano plot (Figure 2A) and clustering heatmap (Figure 2B and Figure S1) revealed 190 significantly downregulated proteins (Table S1) using the standard of fold change ≥ 2 and p value ≤ 0.05 , including lactate dehydrogenase A like 6B (LDHAL6B) and ubiquitin-specific protease 7 (USP7). The differentially expressed proteins

underwent a gene ontology prediction, which showed that spermatid development (biological process), acrosomal vesicle (cellular component) and glycerol kinase activity (molecular function) may participate in busulfan-induced spermatogenesis disorder (Figure 3A and Table S2). KEGG pathway analysis subsequently identified the potential pathways affected by busulfan treatment, such as protein processing in the endoplasmic reticulum, biosynthesis of amino acids, and pyruvate metabolism (Figure 3B and Table S3). Protein interactions were predicted using the STRING database with differentially expressed proteins obtained from proteomics study, which revealed the interaction of spermatogenesis-related proteins such as LDHAL6B/phosducin-like 2 (PDCL2)/lactate dehydrogenase C (LDHC)/protamine 2 (PRM2) (Figure 4) and USP7/tubulin alpha 8 (TUBA8)/ly-1 reactive clone (LYAR)/nuclear autoantigenic sperm protein (NASP) (Figure S2). In addition, predicted protein interactions of LDHAL6B (Figure S3) and USP7 (Figure S4) were conducted using the STRING database with total proteins. 30 days after busulfan treatment, immunofluorescence and western blotting demonstrated that the LDHAL6B (Figures 5, 7A and 7B) and USP7 (Figures S5, S6A and S6B) were significantly reduced in mouse testis. These results indicated that changed expression of LDHAL6B, USP7 and associated proteins in disappearance of most

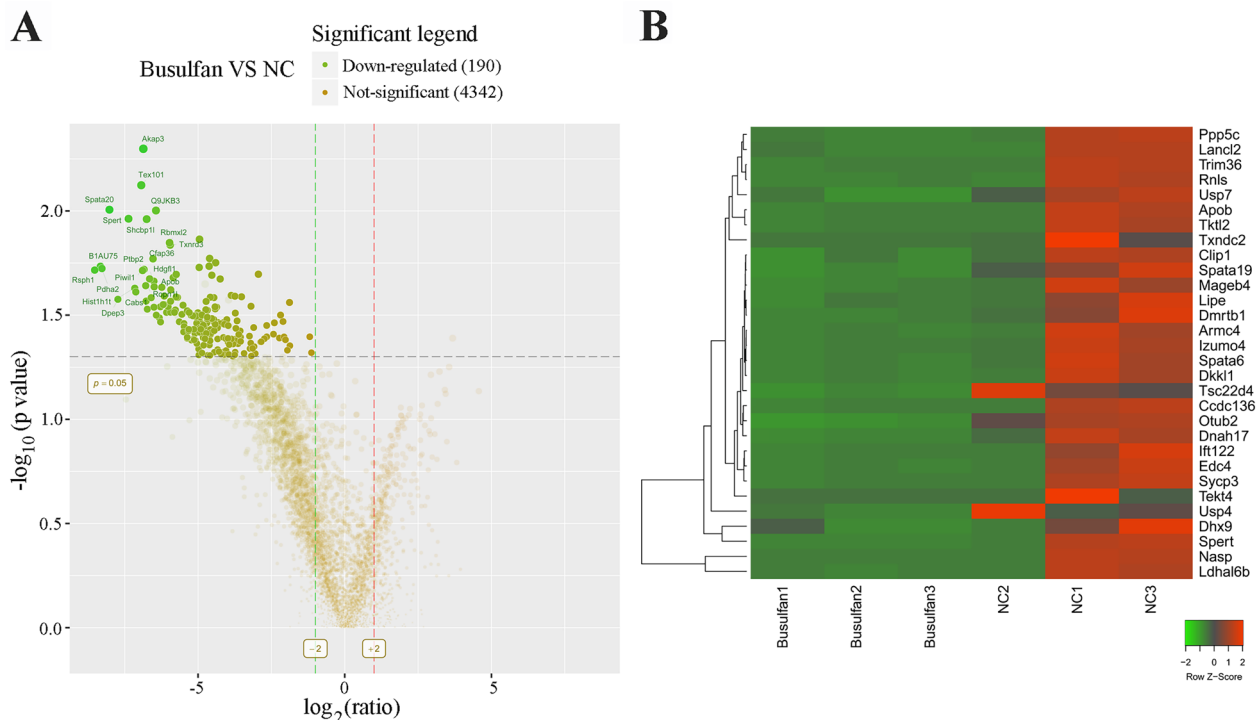


Figure 2. Proteomic analysis of busulfan-treated mouse testis. 190 significantly downregulated proteins were identified in busulfan-treated mouse testis using volcano plot analysis (A). Partially downregulated proteins were shown in the clustering heatmap (B). Mice were injected intraperitoneally once with busulfan, and then testes were separated for label-free quantification proteomics after 30 days. NC, negative control.

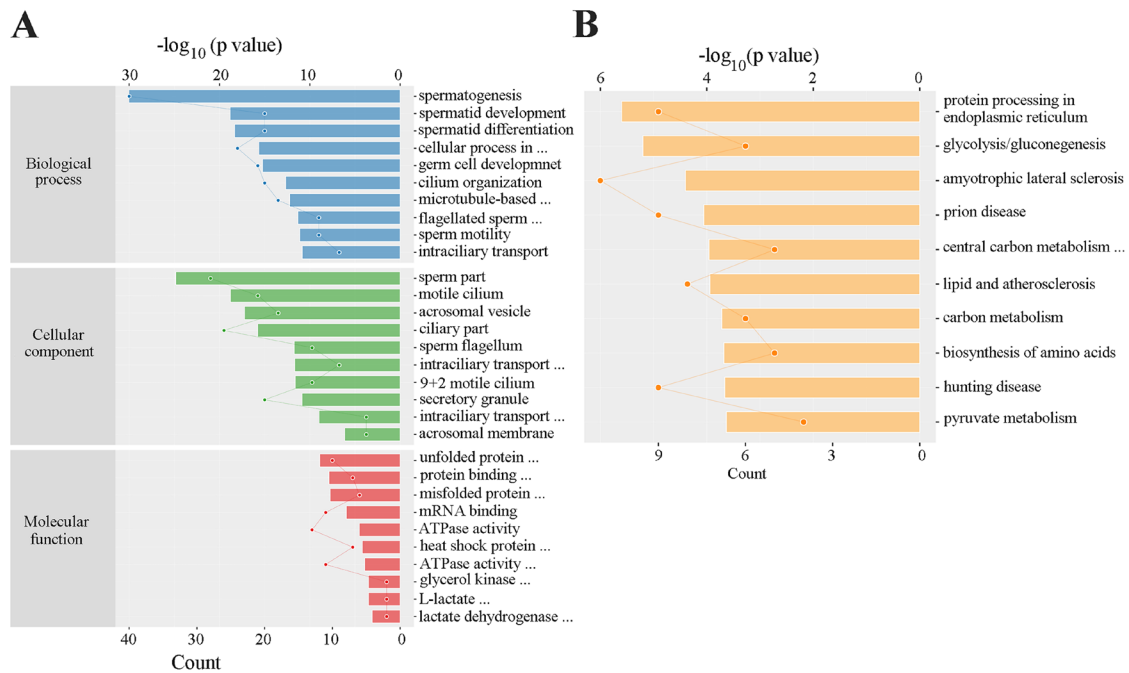


Figure 3. The differentially expressed proteins in busulfan-treated mouse testis were analyzed by bioinformatics. 190 significantly downregulated proteins were analyzed by gene ontology (A) and KEGG pathway analysis (B).

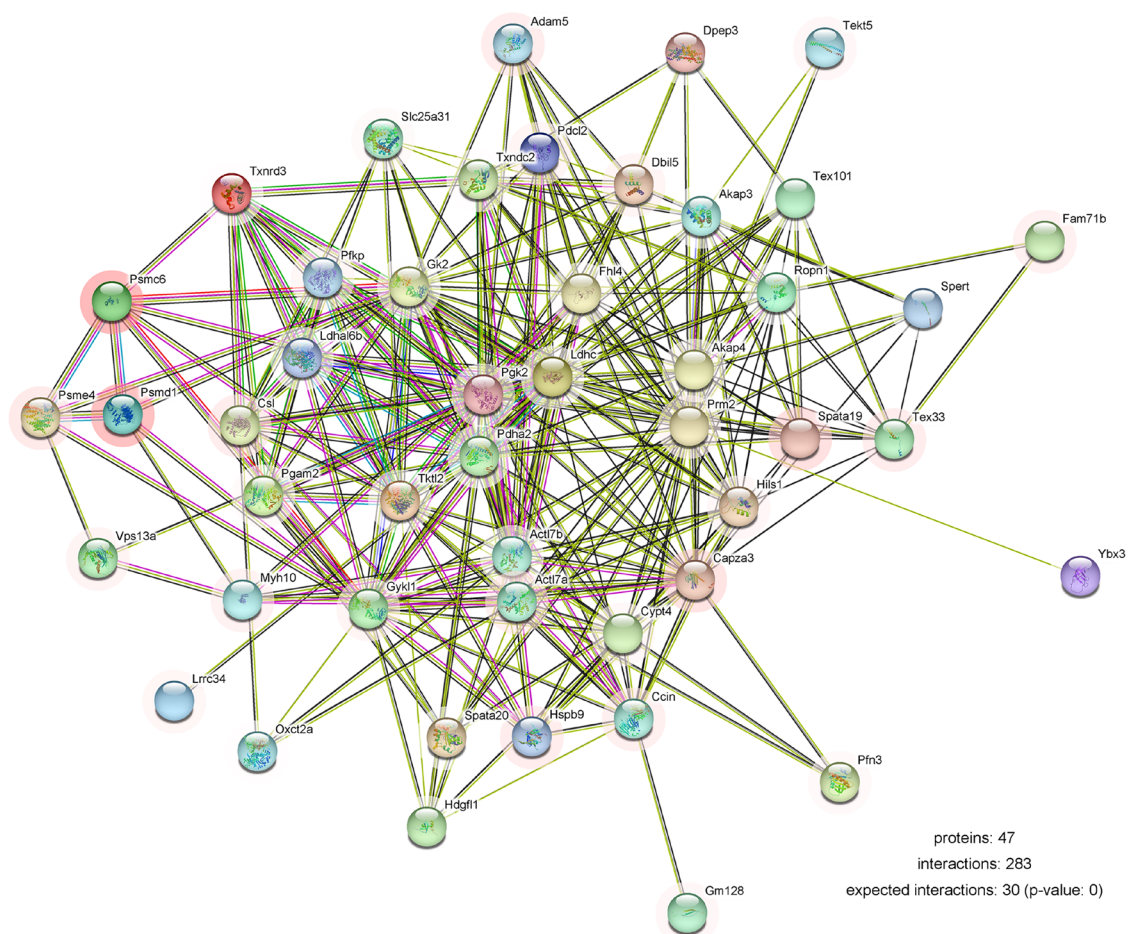


Figure 4. Protein interactions in busulfan-treated testis were analyzed by bioinformatics. Partially downregulated proteins were analyzed using the STRING database. The colored lines show known or predicted interactions of protein. The color for the outer edge of the circle represents difference, and the lighter of the color means the greater of the difference.

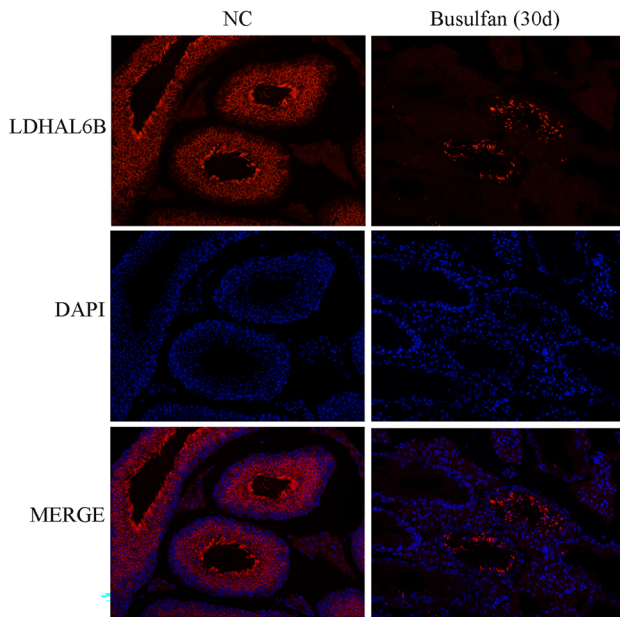


Figure 5. LDHAL6B protein was significantly reduced after 30 days for busulfan-treated mouse testis. Mice were injected intraperitoneally once with busulfan, and then testes were analyzed by immunofluorescence for detection of LDHAL6B protein after 30 days. NC, negative control.

spermatocytes and spermatids in busulfan-induced spermatogenesis disorder.

Spermatogenic recovery in busulfan-treated mouse model

To investigate the spermatogenic recovery of the busulfan-treated mouse model, we examined both molecular and morphological conditions in busulfan-treated mouse testis after 40 to 80 days. The results showed that the testis and spermatozoa in the epididymis progressively improved (Figures 6A and S7) from 70 to 80 days after busulfan treatment, and that the testis weight (Figure 6B) and spermatozoa number (Figure 6C) gradually increased from 40 to 80 days after busulfan treatment. At 80 days after busulfan treatment testicular and sperm recovery was better than 70 days after busulfan treatment (Figure 6 and Figure S7), but more time was needed for spermatogenesis to fully recover. Furthermore, we determined LDHAL6B and USP7 expression in busulfan-induced spermatogenesis disorder mouse testis and found that the protein level of LDHAL6B obviously decreased from 10 to 60 days and increased from 70 to 80 days after busulfan treatment (Figure 7A and 7B) and USP7 protein also showed significant decrease from 30 to 80 days after busulfan treatment (Figure S6A and S6B). Taken together, these results indicated that 70 days is the cut-off point of spermatogenic recovery for busulfan-treated mouse

testis, increasing our understanding of this reproductive disorder model.

Discussion

Recent studies have focused on the omics analyses of testicular effects in the busulfan-induced model [5,18,19]. For example, the aging model of human lung fibroblasts stimulated with busulfan was analyzed by microRNA microarray, which identified some differentially expressed microRNAs that may participate in busulfan-induced aging [19]. Single cell RNA sequencing was performed on the testicular samples treated with busulfan to explore and analyze changes at the molecular and cellular levels [5]. In the current study, busulfan-treated mouse testes were subjected to label-free quantification proteomics, which revealed 190 significantly downregulated proteins. Gene ontology suggested that spermatid development, acrosomal vesicle and glycerol kinase activity may participate in busulfan-induced spermatogenic disorder. KEGG pathway analysis identified the potential pathways affected by busulfan stimulation, including protein processing in endoplasmic reticulum, biosynthesis of amino acids and pyruvate metabolism.

The STRING database revealed that the interaction of the spermatogenesis-related proteins LDHAL6B/PDCL2/LDHC/PRM2 and USP7/TUBA8/LYAR/NASP may be regulated by busulfan. LDHA deficiency in testis resulted in severe defects in spermatogenesis [20]. The protein of LDHAL6B is highly expressed in the brain, heart, lung, urine, skin, ovary and testis [21]. In the testis, LDHAL6B is located in the mitochondria of spermatogenic cells and may play important roles in spermatogenesis [22,23]. In addition, USP7 localizes to the sex chromosome [24] and may play important roles in the normal growth and development of body and physiological functions. The USP7 showed abnormal expression in the oligospermic human semen and can be considered as one of potential molecular markers in the human infertility of oligospermia [25]. PDCL2 is critical for sperm acrosome development and male fertility in mice [26]. TUBA8 shows a strong acrosomal localization and may have a role in spermatid development [27]. LDHC plays crucial roles in maintenance of the processes of glycolysis and ATP production in the sperm flagellum [28]. NASP, a linker histone-binding protein, binds the testis-specific linker histone H1 in the cytoplasm by stimulating ATPase activity and translocate to the nucleus where the H1 is released for binding to the DNA and regulating spermatogenesis [29]. Based on changes in the expression of these proteins, we hypothesize that busulfan mainly destroyed spermatocytes and spermatids through

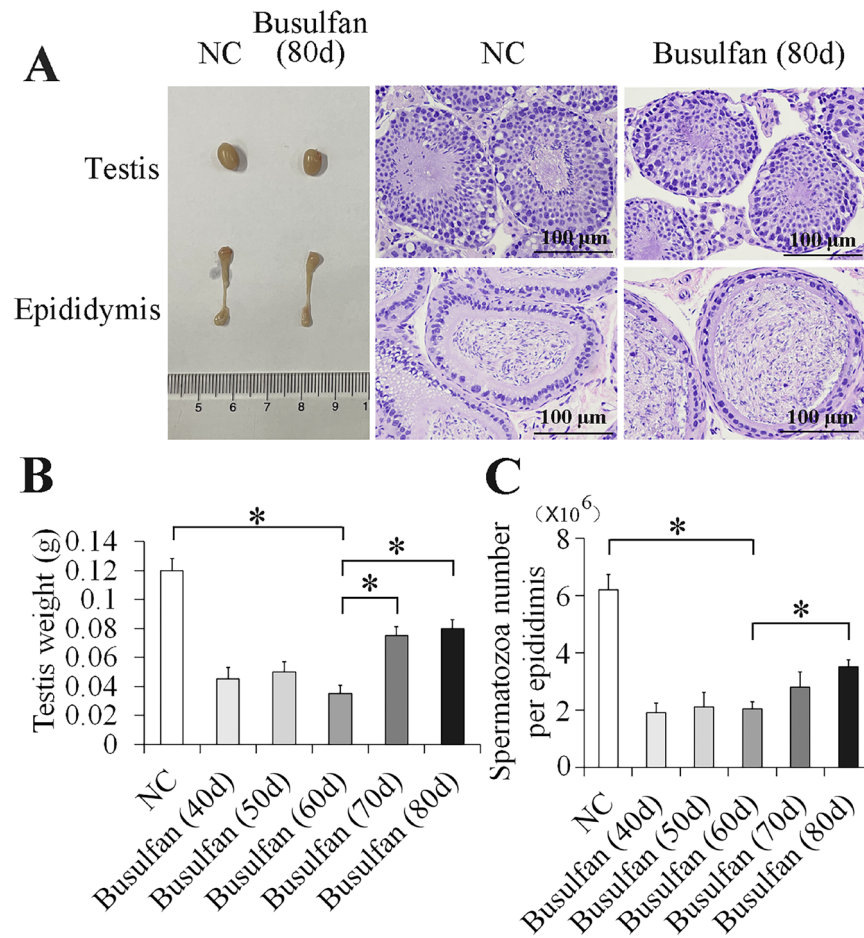


Figure 6. Spermatogenic recovery in busulfan-induced spermatogenesis disorder mouse testis. Recovery of testis and spermatozoa in epididymis progressively improved from 70 days to 80 days after busulfan treatment. Mice were injected intraperitoneally once with busulfan, and then testes and epididymes were separated for morphological imaging and staining with H&E (A), and measurement of testis weight (B) and spermatozoa number (C) after 40, 50, 60, 70 and 80 days. NC, negative control; * $p < 0.05$.

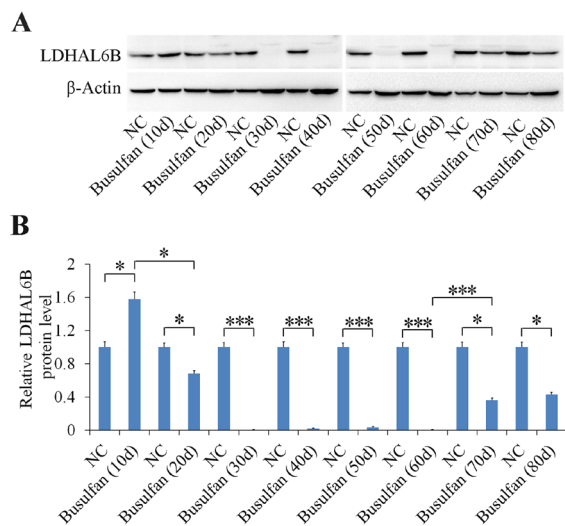


Figure 7. LDHAL6B significantly decreased from 20 to 60 days and increased from 70 to 80 days after busulfan treatment. Mice were injected intraperitoneally once with busulfan, and then testes were separated for detection of LDHAL6B after the specified number of days (A). Densitometry of protein band was analyzed (B). NC, negative control; * $p < 0.05$; *** $p < 0.001$

impairing processes such as energy generation and acrosome formation, which led spermatogenesis disorder in mouse testes. The significantly downregulated proteins in busulfan-treated mouse testes may mediate busulfan-induced reproductive toxicity, which provides guiding value for the clinical use and research of busulfan in the treatment of diseases and reducing the side effects of busulfan.

30 days after busulfan stimulation, we verified that the LDHAL6B and USP7 protein was significantly decreased in mouse testis. In addition, this study revealed that most spermatocytes and spermatids disappeared in busulfan-induced testis. We analyzed LDHAL6B and USP7 expression in busulfan-induced spermatogenesis disorder mouse testis and found that 70 days is the cut-off point of spermatogenic recovery for busulfan-treated mouse testis. The protein expression level of LDHAL6B clearly declined from 10 to 60 days and increased from 70 to 80 days after busulfan treatment and USP7 also showed significant decrease from 30 to 80 days after busulfan treatment, which

indicated that LDHAL6B, USP7 and associated proteins may change dramatically in testis of busulfan-induced spermatogenesis disorder model with disappearance of most spermatocytes and spermatids. LDHAL6B and USP7 might behave as a biomarker for the busulfan treatment during spermatogenesis disorder, which may provide two targets for the effects of the clinical use of busulfan on other tissues and organs. However, the molecular regulatory mechanisms of LDHAL6B/USP7 and associated signaling pathways have not been elucidated in this research, which need to be further studied in future. Testis and spermatozoa in the epididymis progressively improved from 70 to 80 days after busulfan treatment, and that the testis weight and spermatozoa number gradually increased from 40 to 80 days after busulfan treatment. Our research revealed that it takes about 70 days for molecular expression levels to recover and more than 80 days for spermatogenic function and testicular tissue to recover. Taken together, these results indicated that 70 days is the cut-off point of spermatogenic recovery for busulfan-treated mouse testis, increasing our understanding of this reproductive disorder model. The long-term reproductive effects and effects of busulfan on the offspring are still unclear and need to be further studied in future. These findings provide the molecular basis for the clinical application of busulfan and need to be corroborated by future clinical studies.

Conclusion

The model of busulfan-induced mouse spermatogenesis disorder was used to study the protein expression in this study. The damage to the testis and spermatozoa in the epididymis progressively worsened and spermatozoa number also gradually decreased from 10 days to 30 days after busulfan treatment. 30 days after busulfan treatment the mouse testes were subjected to label-free quantification proteomics, which revealed 190 significantly down-regulated proteins. Furthermore, we verified the downregulation of LDHAL6B and USP7 protein from 30 to 80 days after busulfan treatment. We demonstrated that busulfan mainly destroyed spermatocytes and spermatids through impairing processes such as energy generation and acrosome formation. The testis and spermatozoa in the epididymis progressively improved from 70 to 80 days after busulfan treatment, but more time was needed for spermatogenesis to fully recover. These results indicated that 70 days is the cut-off point of spermatogenic recovery for busulfan-treated mouse testis. Further study of busulfan's toxic effect on testes would be beneficial for the treatment of reproductive disorders.

Authors contributions

ML and CS designed the study and wrote the manuscript. KH, QZ, JZ, XL, MY and JY performed the experiments and analyzed the data. SC, FL, BD and SY reviewed the manuscript. All authors have read and approved the manuscript.

Ethics statement

All animal experiments complied with the ARRIVE guidelines and were carried out in accordance with National Regulations on the Control of Laboratory Animals, which was approved by the ethics committee of Bengbu Medical College (Bengbu, China).

Disclosure statement

No potential conflict of interest was reported by the author(s).

Funding

This study was funded by the Key Project of Natural Science Foundation of Anhui Provincial University of China (2023AH052006), the Anhui Provincial Outstanding Young Talents Support Program in Colleges and Universities of China (gxyq2022041), the Anhui Provincial Key Research and Development Project of China (202104j07020016), the Natural Science Research Project of Anhui Educational Committee of China (KJ2020ZD49), the 512 Talent Cultivation Plan of Bengbu Medical College of China (by51201207 and by51201103), and the Climbing Plan of Natural Science General Project of Bengbu Medical College of China (2021bypd003).

ORCID

Ke Hu  <http://orcid.org/0000-0003-3462-5378>
Meng Liang  <http://orcid.org/0000-0003-1641-485X>

Data availability statement

Data for this research are available from the corresponding author (Meng Liang). The mass spectrometry proteomics data for busulfan-treated testis are deposited to the ProteomeXchange Consortium *via* the PRIDE (Perez-Riverol et al. 2022) partner repository with the dataset identifier PXD035492.

References

- [1] Bishop JB, Wassom JS. Toxicological review of busulfan (Myleran). *Mutat Res.* 1986;168(1):15–45. doi: [10.1016/0165-1110\(86\)90020-5](https://doi.org/10.1016/0165-1110(86)90020-5).
- [2] Buggia I, Locatelli F, Regazzi MB, et al. Busulfan. *Ann Pharmacother.* 1994;28(9):1055–1062. doi: [10.1177/106002809402800911](https://doi.org/10.1177/106002809402800911).

- [3] Gouveia HJCB, Manhães-de-Castro R, Costa-de-Santana BJR, et al. Maternal exposure to busulfan reduces the cell number in the somatosensory cortex associated with delayed somatic and reflex maturation in neonatal rats. *J Chem Neuroanat.* 2020;103:101710. doi: [10.1016/j.jchemneu.2019.101710](https://doi.org/10.1016/j.jchemneu.2019.101710).
- [4] Qian C, Meng Q, Lu J, et al. Human amnion mesenchymal stem cells restore spermatogenesis in mice with busulfan-induced testis toxicity by inhibiting apoptosis and oxidative stress. *Stem Cell Res Ther.* 2020;11(1):290. doi: [10.1186/s13287-020-01803-7](https://doi.org/10.1186/s13287-020-01803-7).
- [5] Zhao Y, Zhang P, Ge W, et al. Alginate oligosaccharides improve germ cell development and testicular microenvironment to rescue busulfan disrupted spermatogenesis. *Theranostics.* 2020;10(7):3308–3324. doi: [10.7150/thno.43189](https://doi.org/10.7150/thno.43189).
- [6] Lei B, Xie LX, Zhang SB, et al. Phosphoribosyl-pyrophosphate synthetase 2 (PRPS2) depletion regulates spermatogenic cell apoptosis and is correlated with hypospermatogenesis. *Asian J Androl.* 2020;22(5):493–499. doi: [10.4103/aja.aja_122_19](https://doi.org/10.4103/aja.aja_122_19).
- [7] Kim JE, Nam JH, Cho JY, et al. Annual tendency of research papers used ICR mice as experimental animals in biomedical research fields. *Lab Anim Res.* 2017;33(4):320. doi: [10.5625/lar.2017.33.2.171](https://doi.org/10.5625/lar.2017.33.2.171).
- [8] Hu K, He C, Sun X, et al. Integrated study of circRNA, lncRNA, miRNA, and mRNA networks in mediating the effects of testicular heat exposure. *Cell Tissue Res.* 2021;386(1):127–143. doi: [10.1007/s00441-021-03474-z](https://doi.org/10.1007/s00441-021-03474-z).
- [9] Zhao L, Guo Z, Wang P, et al. Proteomics of epicardial adipose tissue in patients with heart failure. *J Cell Mol Med.* 2020;24(1):511–520. doi: [10.1111/jcmm.14758](https://doi.org/10.1111/jcmm.14758).
- [10] Ashburner M, Ball CA, Blake JA, et al. Gene ontology: tool for the unification of biology. *The Gene Ontology Consortium.* *Nat Genet.* 2000;25(1):25–29. doi: [10.1038/75556](https://doi.org/10.1038/75556).
- [11] Gene Ontology Consortium. The Gene Ontology resource: enriching a GOld mine. *Nucleic Acids Res.* 2021;49(D1):D325–D334. doi: [10.1093/nar/gkaa1113](https://doi.org/10.1093/nar/gkaa1113).
- [12] Mi H, Muruganujan A, Ebert D, et al. PANTHER version 14: more genomes, a new PANTHER GO-slim and improvements in enrichment analysis tools. *Nucleic Acids Res.* 2019;47(D1):D419–D426. doi: [10.1093/nar/gky1038](https://doi.org/10.1093/nar/gky1038).
- [13] Kanehisa M. A database for post-genome analysis. *Trends Genet.* 1997;13(9):375–376. doi: [10.1016/S0168-9525\(97\)01223-7](https://doi.org/10.1016/S0168-9525(97)01223-7).
- [14] Kanehisa M, Furumichi M, Sato Y, et al. KEGG: integrating viruses and cellular organisms. *Nucleic Acids Res.* 2021;49(D1):D545–D551. doi: [10.1093/nar/gkaa970](https://doi.org/10.1093/nar/gkaa970).
- [15] Snel B, Lehmann G, Bork P, et al. STRING: a web-server to retrieve and display the repeatedly occurring neighbourhood of a gene. *Nucleic Acids Res.* 2000;28(18):3442–3444. doi: [10.1093/nar/28.18.3442](https://doi.org/10.1093/nar/28.18.3442).
- [16] Szklarczyk D, Gable AL, Nastou KC, et al. The STRING database in 2021: customizable protein-protein networks, and functional characterization of user-uploaded gene/measurement sets. *Nucleic Acids Res.* 2021;49(D1):D605–D612. doi: [10.1093/nar/gkaa1074](https://doi.org/10.1093/nar/gkaa1074).
- [17] Liang N, Xu Y, Yin Y, et al. Steroidogenic factor-1 is required for TGF-beta3-mediated 17beta-estradiol synthesis in mouse ovarian granulosa cells. *Endocrinology.* 2011;152(8):3213–3225. doi: [10.1210/en.2011-0102](https://doi.org/10.1210/en.2011-0102).
- [18] Badawy AA, El-Magd MA, AlSadrah SA, et al. Altered expression of some miRNAs and their target genes following mesenchymal stem cell treatment in busulfan-induced azoospermic rats. *Gene.* 2020;737:144481. doi: [10.1016/j.gene.2020.144481](https://doi.org/10.1016/j.gene.2020.144481).
- [19] Wang Y, Scheiber MN, Neumann C, et al. MicroRNA regulation of ionizing radiation-induced premature senescence. *Int J Radiat Oncol Biol Phys.* 2011;81(3):839–848. doi: [10.1016/j.ijrobp.2010.09.048](https://doi.org/10.1016/j.ijrobp.2010.09.048).
- [20] Zhang XN, Tao HP, Li S, et al. Ldha-dependent metabolic programs in sertoli cells regulate spermiogenesis in mouse testis. *Biology (Basel).* 2022;11(12):1791. doi: [10.3390/biology11121791](https://doi.org/10.3390/biology11121791).
- [21] Samaras P, Schmidt T, Frejno M, et al. ProteomicsDB: a multi-omics and multi-organism resource for life science research. *Nucleic Acids Res.* 2020;48(D1):D1153–D1163. doi: [10.1093/nar/gkz974](https://doi.org/10.1093/nar/gkz974).
- [22] Mostek-Majewska A, Janta A, Majewska A, et al. Effect of 2-Cys peroxiredoxins inhibition on redox modifications of bull sperm proteins. *Int J Mol Sci.* 2021;22(23):12888. doi: [10.3390/ijms222312888](https://doi.org/10.3390/ijms222312888).
- [23] Wang H, Zhou Z, Lu L, et al. Cloning and characterization of a novel intronless lactate dehydrogenase gene in human testis. *Int J Mol Med.* 2005;15(6):949–953. doi: [10.3892/ijmm.15.6.949](https://doi.org/10.3892/ijmm.15.6.949).
- [24] Menon DU, Shibata Y, Mu W, et al. Mammalian SWI/SNF collaborates with a polycomb-associated protein to regulate male germline transcription in the mouse. *Development.* 2019;146(19):dev174094. doi: [10.1242/dev.174094](https://doi.org/10.1242/dev.174094).
- [25] Farahani M, Yaghobi Z, Ramezani M, et al. USP7 and SET9 expression in the oligospermic human semen: a case-control study. *Int J Fertil Steril.* 2022;16(4):306–309. doi: [10.22074/ijfs.2021.537310.1174](https://doi.org/10.22074/ijfs.2021.537310.1174).
- [26] Fujihara Y, Kobayashi K, Abbasi F, et al. PDCL2 is essential for sperm acrosome formation and male fertility in mice. *Andrology.* 2023;11(5):789–798. doi: [10.1111/andr.13329](https://doi.org/10.1111/andr.13329).
- [27] Diggle CP, Martinez-Garay I, Molnar Z, et al. A tubulin alpha 8 mouse knockout model indicates a likely role in spermatogenesis but not in brain development. *PLoS One.* 2017;12(4):e0174264. doi: [10.1371/journal.pone.0174264](https://doi.org/10.1371/journal.pone.0174264).
- [28] Odet F, Duan C, Willis WD, et al. Expression of the gene for mouse lactate dehydrogenase C (Ldhc) is required for male fertility. *Biol Reprod.* 2008;79(1):26–34. doi: [10.1095/biolreprod.108.068353](https://doi.org/10.1095/biolreprod.108.068353).
- [29] Alekseev OM, Widgren EE, Richardson RT, et al. Association of NASP with HSP90 in mouse spermatogenic cells: stimulation of ATPase activity and transport of linker histones into nuclei. *J Biol Chem.* 2005;280(4):2904–2911. doi: [10.1074/jbc.M410397200](https://doi.org/10.1074/jbc.M410397200).